
Use of an Aggressive MCF-7 Cell Line Variant, TMX2-28, to Study Cell Invasion in Breast Cancer

Joseph M. Gozgit,¹ Brian T. Pentecost,² Sharon A. Marconi,³ Christopher N. Otis,³ Chuanyue Wu,⁴ and Kathleen F. Arcaro¹

¹Department of Veterinary and Animal Sciences, University of Massachusetts, Amherst, Massachusetts; ²Wadsworth Center, New York, State Department of Health, Albany, New York; ³Department of Pathology, Baystate Medical Center, Springfield, Massachusetts; and ⁴Department of Pathology, University of Pittsburgh, Pittsburgh, Pennsylvania

Abstract

An estrogen receptor–negative variant of the MCF-7 breast cancer cell line, TMX2-28, was used as a model in which to study breast cancer cell invasion. Using a reconstituted basement membrane (Matrigel) assay to evaluate cell invasion, we determined that TMX2-28 cells are more invasive than MCF-7 cells and that the invasiveness of TMX2-28 is similar to that of the aggressive MDA-MB-231 breast cancer cell line. TMX2-28 cells displayed a rounded, epithelial cell–like morphology, suggesting an amoeboid mode of cell invasion, in contrast to the mesenchymal mode of invasion characteristic of spindle-shaped, fibroblast-like MDA-MB-231 cells. Using real-time reverse transcription-PCR, we found that mitogen-inducible gene 2 (*MIG2*) is expressed at a 17-fold higher level in TMX2-28 cells than in nonaggressive MCF-7 cells and that *MIG2* mRNA levels are low in the nontumorigenic human mammary epithelial cell line, 184. We determined that *MIG2* plays a role in cell invasion by using small interfering RNA (siRNA) to suppress the expression of *MIG2* mRNA levels in TMX2-28 cells. TMX2-28 cell invasion was reduced by 48% when the cells were transfected with siRNAs targeting *MIG2*, relative to cells transfected with siRNAs against glyceraldehyde-3-phosphate dehydrogenase. Finally, *MIG2* expression was evaluated in reductive mammoplasty and breast tumor tissue. Although all 21 normal tissues from reduction mammoplasty showed immunoreactivity for *MIG2*, ranging from weak (62%) to strong (24%), only half of the 34 formalin-fixed breast tumors showed immunoreactivity for *MIG2*. Of these 17 positive cases, 10 were considered to overexpress *MIG2* (moderate to strong staining). Examination of 30 frozen breast tumors

supported the finding that *MIG2* is overexpressed in a subset of breast cancers. We suggest that *MIG2*'s normal regulation and function are disrupted in breast cancer. (*Mol Cancer Res* 2006;4(12):905–13)

Introduction

Metastasis is a hallmark of the cancer phenotype and accounts for 90% of cancer deaths (1). Breast cancer is among the four most common cancers (2), and aggressive breast cancers frequently metastasize to the lungs and bones (3). However, metastasis is a relatively inefficient process, and it is thought that tumor cells must acquire a phenotypic advantage before they can proceed through the metastatic cascade (4–6). Cancer cell invasion is an essential process in the metastatic cascade. Tumor cells must invade surrounding extracellular matrix (ECM) tissues to enter the lymphatic and circulatory systems for dissemination to distant sites in the body, and it is thought that proteins controlling cell-ECM interactions play a role in this process (4, 5, 7–10). Studies have shown that cancer cells must acquire a motility or invasion gene expression signature if they are to convert to the invasive phenotype (reviewed in ref. 9), and recently, it has been shown that cancer cells can invade by multiple mechanisms such as mesenchymal or amoeboid motilities (7, 9, 11). A mesenchymal type of motility is characteristic of elongated, fibroblast-like cells that are proteolysis-dependent for tissue remodeling and path generation; in contrast, an amoeboid type of motility is characteristic of roundish or ellipsoid cells that propel themselves through tissue in a proteolysis-independent manner, by squeezing through narrow regions. An important consideration for targeting cancer cell invasion as part of breast cancer treatment will be to develop models to investigate the mechanisms that control these contrasting types of cell invasion.

The mitogen-inducible gene 2 (*MIG2*) was first identified as a serum-inducible gene by differential cDNA screening in the human diploid fibroblast cell line, WI-38 (12). *MIG2* belongs to a newly recognized protein family comprising URP1, URP2 and the *Caenorhabditis elegans* protein, UNC-112, which all share a unique protein structure consisting of two 4.1-ezrin-radixin-moesin domains flanking a pleckstrin homology domain (13, 14). *MIG2* has been further characterized as a component of cell-ECM adhesion sites and described its involvement in controlling cell shape and spreading (15). Using yeast two-hybrid screening, those authors showed that

Received 5/23/06; revised 9/25/06; accepted 10/16/06.

Grant support: NIEHS grants R01 ES09795 and K02 ES000384 (K. Arcaro), and NIH grant GM65188 (C. Wu).

The costs of publication of this article were defrayed in part by the payment of page charges. This article must therefore be hereby marked advertisement in accordance with 18 U.S.C. Section 1734 solely to indicate this fact.

Requests for reprints: Kathleen F. Arcaro, 639 North Pleasant Street, Morrill 1 North, RM N422, Amherst, MA 01003. Phone: 413-577-1823; Fax: 413-545-5731. E-mail: karcaro@nre.umass.edu

Copyright © 2006 American Association for Cancer Research.
doi:10.1158/1541-7786.MCR-06-0147

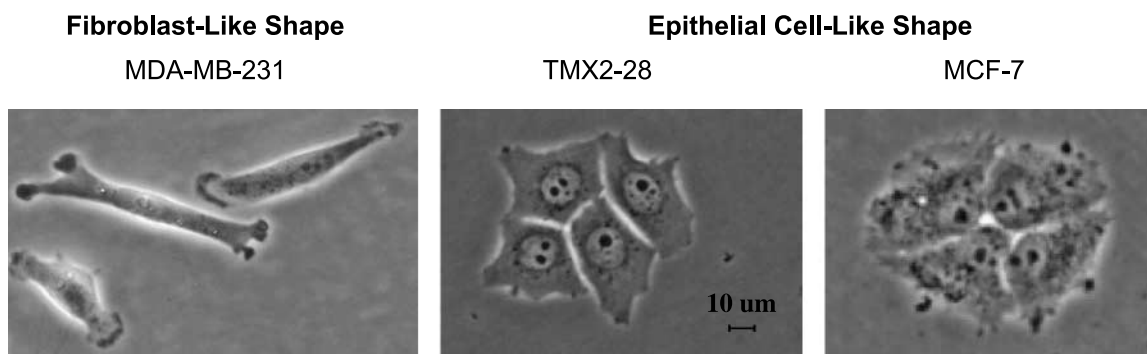


FIGURE 1. TMX2-28 cells maintain a roundish cell morphology similar to that of MCF-7. Phase-contrast microscopy and QCapture Pro3 software were used to photograph and measure the cell dimensions of TMX2-28, MCF-7, and MDA-MB-231 cells grown under standard culture conditions.

MIG2 interacts with a recently characterized LIM domain-containing protein that they termed migfilin (15). MIG2 recruits migfilin to cell-ECM adhesions, forming a complex with the actin cross-linking protein, filamin, and promoting cellular dynamics through the interaction with the actin cytoskeleton. Furthermore, migfilin localizes to cell-cell junctions, in a MIG2-independent manner, and is involved in maintaining the organization of adherens junctions (16).

In this study, we have used a novel cell line, TMX2-28, which was clonally derived from the human MCF-7 breast cancer cell line following prolonged cultivation in the presence of the antiestrogen, tamoxifen (17). We first characterized the invasive phenotype of TMX2-28 cells, by comparing them to nonaggressive MCF-7 cells and to aggressive, fibroblast-like MDA-MB-231 cells. Then, using gene expression analysis, we identified the overexpression of MIG2 in TMX2-28 breast cancer cells and found that silencing MIG2 by small interfering RNAs (siRNA) reduced TMX2-28 cell invasion. Last, we found that although MIG2 protein was detected in all 21 of the reductive mammaplasty tissues examined, it was detected in only half of the 34 tumor samples examined. Furthermore, MIG2 mRNA levels were high in only 9 of 30 additional tumor samples, suggesting that the regulation of MIG2 was disrupted in breast cancers.

Results

Phenotypic Characterization of TMX2-28 Cells

The TMX2-28 cell line was clonally derived from the human MCF-7 breast cancer cell line following prolonged cultivation in the presence of the antiestrogen, tamoxifen. TMX2-28 cells have lost expression of the estrogen receptor (17, 18) and they express a mixed basal/luminal cytokeratin profile.⁵ TMX2-28 cells maintain a rounded epithelial morphology similar to that of MCF-7 cells, which is in contrast to the fibroblast, spindle-like morphology of MDA-MB-231 breast cancer cells (Fig. 1). To quantify the difference in cell morphology between TMX2-28 and MDA-MB-231 cells, we took still-frame photographs and measured cell dimensions. The length-to-width ratios

showed the similar rounded morphologies of TMX2-28 and MCF-7 (L/W ratio of 1.1 ± 0.09 SD, $n = 10$; and 1.3 ± 0.22 SD, $n = 10$, respectively). In contrast, MDA-MB-231 cells were elongated (L/W ratio of 6.2 ± 1.6 SD, $n = 10$). We used a reconstituted basement membrane (Matrigel) to evaluate the cell invasion potential of TMX2-28 cells, and to compare them to the highly invasive MDA-MB-231 cells and the noninvasive MCF-7 parent cells. Cell migration was determined by the number of cells that moved from the top to the bottom of the porous membrane, whereas in cell invasion, the cells had to invade through the barrier of the Matrigel layer. Figure 2A shows representative photomicrographs of cells that were fixed and stained on the bottom of either control or Matrigel-layered porous membranes. Quantification of the number of stained cells revealed that TMX2-28 and MDA-MB-231 cells migrated similarly, and that both cell lines migrated much faster compared with MCF-7 cells (Fig. 2B, left). TMX2-28 cells invaded to an only slightly lesser extent (nonstatistical, $P > 0.05$) compared with the aggressive MDA-MB-231 cells; more importantly, TMX2-28 cells invaded through the Matrigel, whereas MCF-7 cells did not (Fig. 2B, right).

MIG2 Expression in Breast Cancer Cell Lines

To determine whether TMX2-28 cells differentially express genes involved in cell adhesion and cell-ECM interactions, we analyzed cDNA microarray data from a comparison of MCF-7 and TMX2-28 cells on the Affymetrix Human Genome U133 Plus 2.0 Array. The cDNA microarray comparison of TMX2-28 and MCF-7 cells identified 1,402 differentially expressed transcripts, among which 200 transcripts were up-regulated.⁵ Using NetAffx analysis (Affymetrix, Santa Clara, CA; ref. 19), we identified several cell membrane, adhesion, and cell-ECM-associated genes that were up-regulated in TMX2-28 cells (Table 1). MIG2 is localized to focal adhesions and plays a role in controlling actin cytoskeleton dynamics (15); therefore, it is probable that MIG2 plays a role in promoting cell motility and invasion. Tu and colleagues (15) examined the expression of MIG2 in a variety of cell types and found that MIG2 was at a relatively low level in MCF-7 cells. We thought it was intriguing that MIG2 was overexpressed in TMX2-28 breast cancer cells; and therefore, further investigated the expression and function of MIG2 in breast cancer. Using real-time reverse transcription-PCR, we confirmed the level of MIG2 mRNA in

⁵J.M. Gozgit, C.N. Otis, B.T. Pentecost, S.A. Marconi and K.F. Arcaro. PLD1 is overexpressed in a subset of phospho-Akt-negative breast carcinomas: Biomarker for alternative mTOR activation. Submitted.

TMX2-28 cells and found that it was ~17-fold higher than in either MCF-7 cells or the nontumorigenic human mammary epithelial cells (HMEC) finite life span 184 cell line (Fig. 3A). As shown in Fig. 3B, the protein expression profiles for MIG2 in TMX2-28, MCF-7, and 184 cells are similar to the mRNA expression profiles. We found that MIG2 mRNA levels vary among a panel of breast cancer cell lines with different degrees of invasiveness and among different nontumorigenic breast cell lines; however, MIG2 is expressed significantly more highly in TMX2-28 cells ($P < 0.05$) compared with any of the other cell lines (Fig. 3C). Higher MIG2 mRNA expression (>0.2 arbitrary units; Fig. 3C) was observed in three of seven cancer cell lines and in none of the five the nontumorigenic HMEC lines.

MIG2 Is Serum-Inducible in HMECs

MIG2 was first identified in the human diploid fibroblast cell line WI-38 as a serum-inducible gene (12). MIG2 is endogenously highly expressed in the MCF-7 cell variant, TMX2-28, under normal growth conditions (i.e., 5% cosmic calf serum); MCF-7 cells are a hormone-sensitive cell line, therefore, we examined whether *MIG2* gene expression was induced following either serum or estrogen stimulation in MCF-7 cells and HMECs. MIG2 mRNA levels were not significantly induced in MCF-7 ($P > 0.05$) cells following a 4 or 24 h treatment with either 10% fetal bovine serum (FBS) or 1 nmol/L E_2 (Fig. 4, *lined columns*). To determine whether MIG2 is inducible in nontumorigenic breast cells, we evaluated MIG2 expression in HMECs. In contrast to MCF-7 cells, MIG2 mRNA levels in HMECs were significantly ($P < 0.05$) induced by 7-fold, following 4 h of treatment with 10% FBS (Fig. 4, *white columns*).

MIG2 and Cell Invasion by TMX2-28 Cells

We have found that MIG2 is overexpressed in aggressive TMX2-28 cells compared with nonaggressive cancer cell lines and nontumorigenic HMECs. This finding, together with the previous demonstration that MIG2 is localized to focal adhesions and plays a role in controlling actin cytoskeleton dynamics (15), prompted us to investigate the role of MIG2 in TMX2-28 cell invasion. Using transient transfection of siRNAs targeting MIG2, we silenced MIG2 expression by 52% relative to the negative control (siRNAs targeting glyceraldehyde-3-phosphate dehydrogenase, GAPDH; Fig. 5A and C). TMX2-28 cells were transfected with siRNAs, and 48 h later, were collected and placed in the upper half of either the control membrane inserts or Matrigel-layered inserts, which were then incubated for a further 24 h. Representative photomicrographs of cells that were fixed and stained illustrate that TMX2-28 cells transfected with GAPDH siRNAs migrate and invade faster compared with cells transfected with MIG2 siRNAs (Fig. 5B). Following the quantification of stained cells, the percentage of invasion was calculated by normalization of the number of cells that invaded through the Matrigel layer, to the number of cells that migrated through the control membrane without Matrigel. This measure takes into account the changes in cell health and viability resulting from cytotoxicity encountered during the transfection. The percentage of invasion is shown in Fig. 5D as box and whisker plots illustrating the 10th, 25th, median, 75th, and 90th percentiles for both GAPDH and MIG2 siRNA-treated cells. The box and whisker plots show the variability among five experiments, however, each experiment showed an ~2-fold (48%) lower invasiveness of TMX2-28 cells treated with MIG2 siRNAs than in cells treated

FIGURE 2. TMX2-28 cells are highly invasive compared with MCF-7 cells. A reconstituted basement membrane (Matrigel) assay was used to determine the invasion potentials of three breast cancer cell lines. Cells were seeded into either a porous 8 μ m membrane insert (control) or Matrigel-layered membrane insert, and incubated over a chemoattractant (5% FBS) for 24 h. Cells were fixed on the membrane, stained, photographed, and counted. Representative images of cells that migrated through the membrane and invaded through the Matrigel layer (A). Five frames were counted and graphed for cell migration and invasion. Columns, means from one representative experiment indicating the variability among the five frames counted across the area of the membrane; bars, SD. Experiments were repeated four times with similar results. Statistical significance was determined using one-way ANOVA with Bonferroni's post hoc *t* test (B).

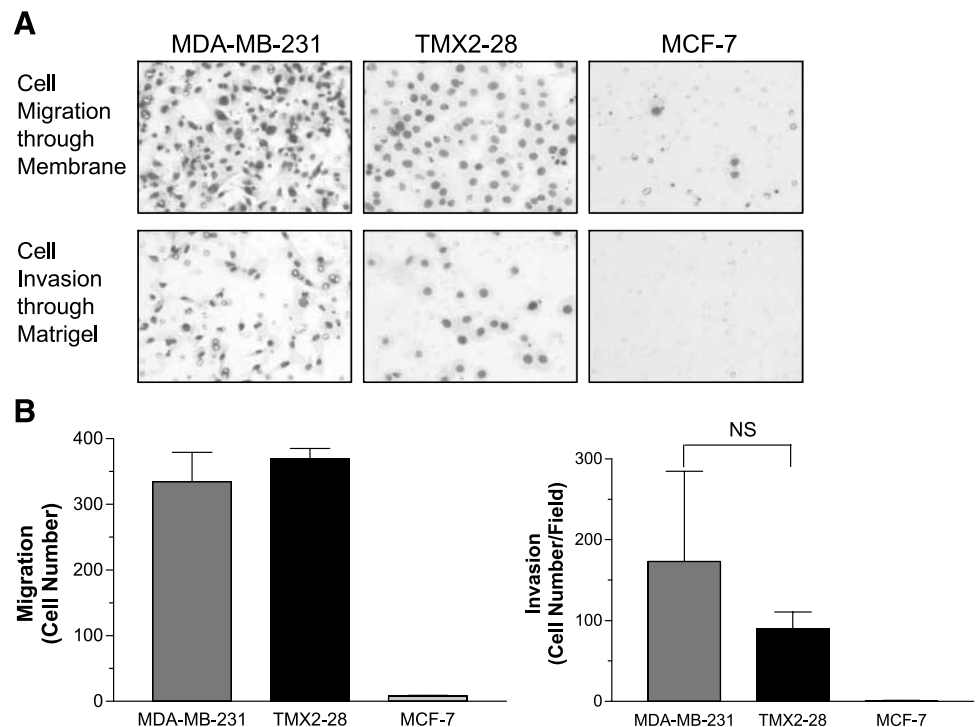


Table 1. Genes Associated with Cell Cytoskeleton, Adhesion, or Plasma Membrane That Were Up-Regulated in the TMX2-28 Cell Line as Compared with the Parent MCF-7 Cell Line

Gene name and GO function	Symbol	GenBank	Fold change	
			Array	QPCR
Cytoskeleton				
Mitogen inducible gene 2	<i>MIG2</i>	NM_006832	2.3	17
Dystonin	<i>DST</i>	NM_001723	2.0	1.5
Sarcoglycan ϵ	<i>SGCE</i>	NM_003919	2.3	not tested
CDC42 effector protein 3	<i>CDC42EP3</i>	NM_006449	2.5	not tested
Cell adhesion				
Laminin γ 1	<i>LAMC1</i>	NM_002293	2.0	21
Laminin β 1	<i>LAMB1</i>	NM_002291	2.1	12
Collagen type XXI α 1	<i>COL21A1</i>	NM_030820	3.2	46
Vitronectin	<i>VTN</i>	NM_000638	2.1	>100
Parvin α	<i>PARVA</i>	NM_018222	2.0	5.0
Desmocollin 2	<i>DSC2</i>	NM_024422	2.8	>100
Calsyntenin 3	<i>CLSTN3</i>	NM_014718	2.8	not tested
Semaphorin 5A	<i>SEMA5A</i>	NM_003966	2.0	not applicable
Plasma membrane				
Paralemmin	<i>PALM</i>	NM_002579	2.5	8.0
Phospholipase C-like protein 2	<i>PLCL2</i>	NM_015184	2.1	>100
Dipeptidase 2	<i>DPEP2</i>	NM_022355	14	>100
CD31	<i>PECAMI</i>	NM_000442	2.1	>100

NOTE: GO, gene ontology biological process determined from NetAffx; Array, results from cDNA microarray comparison of TMX2-28 and MCF-7 cells; QPCR, results from real-time reverse transcription-PCR test between TMX2-28 and MCF-7 cells.

with GAPDH siRNAs. Analysis of results from five experiments showed that mean invasiveness was significantly lower in TMX2-28 cells treated with siRNA targeting MIG2 (22.3%) than in TMX2-28 cells treated with siRNA targeting GAPDH (46.3%, one-tailed *t* test, $P < 0.05$).

MIG2 Expression in Human Normal and Cancer Breast Tissues

To determine whether MIG2 was expressed in clinical breast cancer specimens, we collected archived human breast carcinomas from Baystate Medical Center (Springfield, MA). We evaluated *MIG2* gene expression in RNA isolated from 30 frozen breast tumors and found that MIG2 mRNA was overexpressed (>0.2 arbitrary units) in 9 of the 30 (30%) breast tumors (Fig. 6). We found no significant association between MIG2 expression and tumor grade, however, there was a trend for MIG2 to be more highly expressed in grades 1 and 2 as opposed to grade 3 tumors. Using tissue microarray (TMA) and immunohistochemistry, we evaluated MIG2 protein expression in 34 breast tumor and 21 reduction mammoplasty formalin-fixed, paraffin-embedded (FFPE) tissues. Figure 7 shows MIG2-positive (Fig. 7A) and MIG2-negative (Fig. 7C) expression from a representative TMA core sample and magnified image. We found that MIG2 shows variable, either high or low, expression in tissues from reduction mammoplasty as shown in Fig. 7B and D, respectively. Table 2 presents the results from immunohistochemical analysis showing the immunoreactivity of MIG2. MIG2 protein was expressed in 17 of 34 (50%) breast carcinomas tested. Of the 17 tumors that showed positive MIG2 immunoreactivity, more than half (9 of 17) showed moderate to strong staining. As with the mRNA levels, there was no significant association between tumor grade and MIG2 protein expression, however, there was a trend for MIG2 to be more highly expressed in grades 1 and 2 tumors as opposed to grade 3 tumors. In contrast to the tumor tissue,

staining for MIG2 was positive in all 21 reductive mammo-plasties tested. Thirty-eight percent of the reduction mammo-plasties showed moderate to strong staining, and the remaining 62% of the tissues showed weak immunoreactivity.

Discussion

In this report, we introduce a novel cell line, TMX2-28, in which to study estrogen receptor-negative, invasive breast cancer. The majority of studies using cell cultures to study breast cancer cell invasion have used the fibroblast-like MDA-MB-231 cell line as a model. To the best of our knowledge, the TMX2-28 cell line used here is the only non-genetically engineered line in which cells are estrogen receptor-negative, display a rounded, epithelial cell-like morphology, and are highly invasive. Cell invasion is an essential process in the metastatic cascade, and therefore proteins controlling this process are attractive therapeutic targets. Recently, it was shown that cancer cells could use alternative mechanisms of motility for cell invasion (7, 11). Matrix metalloproteinases (MMP) are a group of proteases that degrade ECM components and are thought to play a role in cancer cell invasion. However, results from clinical trials have shown that MMP inhibitors are unsuccessful in preventing the growth of late-stage metastatic tumors (reviewed in refs. 9, 20). Wolf and colleagues reported that fibroblast-like, spindle-shaped MDA-MB-231 breast cancer cells revert to a roundish, epithelial cell-like morphology during cell invasion, when challenged with MMP inhibitors (7, 11). Those authors suggested that the cells acquire an alternative mechanism of cell invasion that is no longer dependent on proteolytic degradation of ECM components but instead is dependent on propulsion. Interestingly, the majority of cancer cells in solid tumors do not undergo an epithelial-to-mesenchymal transition, and they must therefore invade tissue using mechanisms other than the mesenchymal mode of cell motility (reviewed in ref. 9). These observations

suggest that it is important to understand the alternative mechanisms of cell invasion if we are to efficiently target this process. Data from our studies show that TMX2-28 cells are highly invasive relative to MCF-7 cells and maintain a rounded epithelial morphology, which suggests that TMX2-28 cells may use an amoeboid type of cell motility for invasion.

Several studies have identified genes that are overexpressed in invasive cancer cells, and it is thought that cells which acquire this invasion signature form highly metastatic tumors

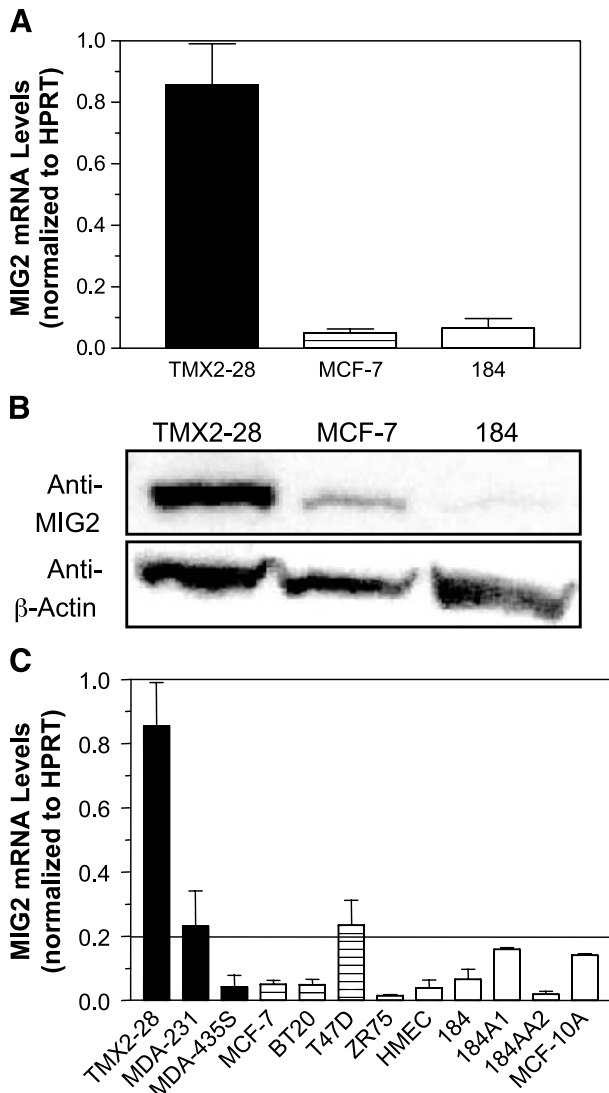


FIGURE 3. MIG2 is overexpressed in TMX2-28 breast cancer cells. RNA was isolated from cell cultures, and gene expression was determined using real-time reverse transcription-PCR. Columns, means from two biological samples each tested in duplicate and normalized to hypoxanthine ribosyltransferase; bars, SD (A). Protein lysates (10 μ g) isolated from cell cultures were probed for MIG2 expression by Western immunoblotting; the experiment was repeated thrice with different biological samples (B). Gene expression was determined from RNA isolated from a panel of cell lines: black columns, aggressive; lined columns, nonaggressive; white columns, nontumorigenic. Relative mRNA levels >0.2 arbitrary units were considered overexpressed (above the solid line). Statistical significance was determined using a one-way ANOVA with Bonferroni's post hoc *t* tests (C).

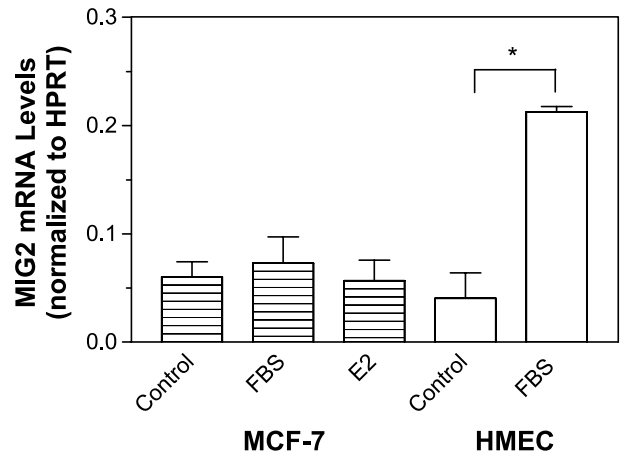


FIGURE 4. MIG2 is induced in HMECs following serum stimulation. MCF-7 cells (lined columns) and HMECs (white columns) were grown in basal medium for 48 hours and then treated with either control medium (DC₅ or mammary epithelial growth medium), medium with 10% FBS, or serum-free medium containing 1 nmol/L E₂ for 4 hours before RNA was isolated (see text for details). Columns, means from two experiments normalized to hypoxanthine ribosyltransferase; bars, SD. Statistical significance was determined using a one-way ANOVA and Bonferroni's post hoc *t* test.

(9, 10, 21, 22). Data from these studies have also identified genes that are involved in cell adhesion and cell-ECM interactions as important components of the cell invasion process. TMX2-28 cells differ from MCF-7 cells in the types of ECM components that they secrete. As shown in Table 1, TMX2-28 cells express mRNA for various laminin and collagen subunits, which are, interestingly, also highly expressed in basal-like HMECs. TMX2-28 cells also overexpress mRNAs for many cell membrane morphoregulatory genes and genes that control cytoskeletal organization. The cDNA microarray comparison of MCF-7 and TMX2-28 cells revealed no differences in the mRNA levels of the major matrix MMPs (-1, -2, -8, and -13); however, three proteases, MMP-like 1, and cathepsins F and S, were down-regulated in the TMX2-28 cell line by ~3-fold. We did find that tissue inhibitors of metalloproteinases-1 and -2 are down-regulated in the TMX2-28 cell line. Further investigation of MMPs and MMP inhibitors in TMX2-28 cells is warranted.

In this study, we identified the expression of MIG2 in breast carcinomas and found that it plays a role in breast cancer cell invasion in cell culture. MIG2 has previously been reported to be overexpressed in uterine leiomyomas, relative to normal myometrium (23). The authors speculated that MIG2 is overexpressed on the transcriptional level, and that MIG2 could be involved in hormone-mediated growth. Weinstein and colleagues found that expression patterns for the three protein family members, MIG2, URP1, and URP2 differed among various tumor tissues (13). The authors reported that URP1 expression was increased in 70% of colon and 60% of lung carcinomas, but was not increased in breast carcinomas. MIG2 expression was increased in 2 of 10 breast carcinomas and in 1 of 10 lung carcinomas, whereas the expression of URP2 was unchanged in all of the cancer tissues examined. We found that MIG2 is more highly expressed in aggressive TMX2-28 breast

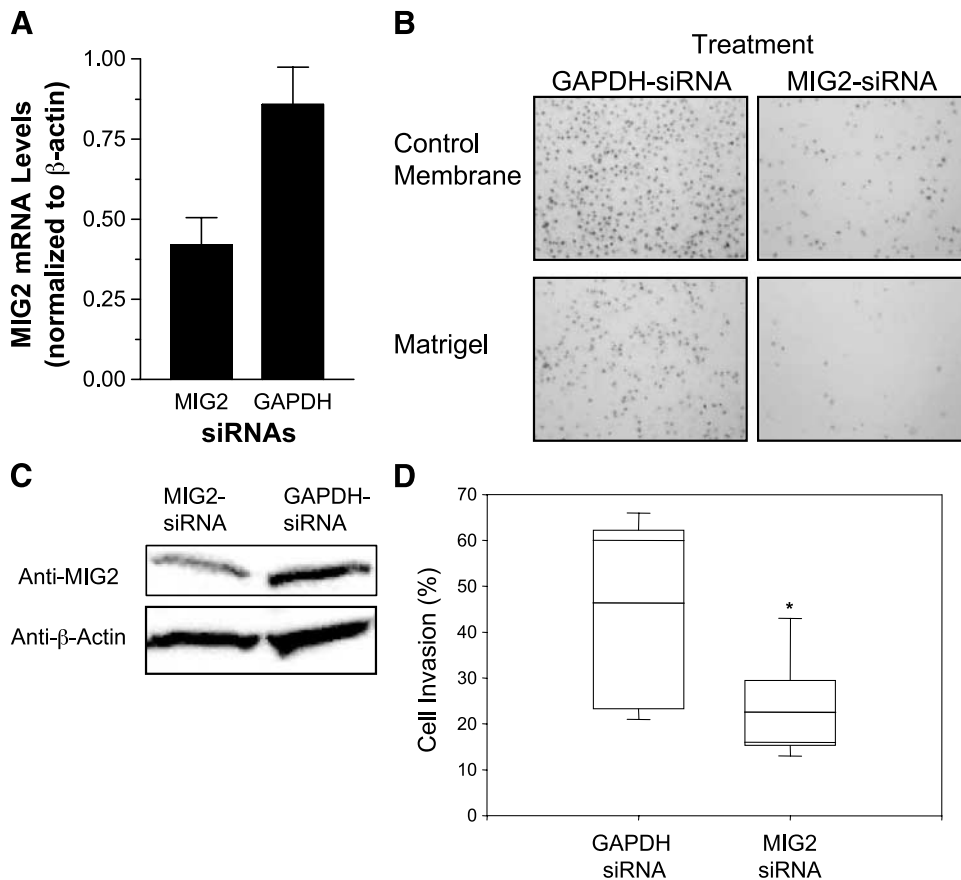


FIGURE 5. siRNA-mediated suppression of MIG2 reduces TMX2-28 cell invasion. TMX2-28 cells were transiently transfected with siRNAs targeting either MIG2 or GAPDH (negative control) for 72 h, before RNA and protein were purified and measured for MIG2 expression by either real-time reverse transcription-PCR (**A**) or Western immunoblotting (**C**). TMX2-28 cells transfected with either GAPDH or MIG2 siRNA were assayed for cell invasion using the Matrigel assay 48 h posttransfection. Representative images of stained cells that either migrated through the porous control membrane or invaded through the Matrigel-layered membrane (**B**). The number of cells that invaded through the Matrigel were normalized to the number of cells that migrated through the control membrane and are shown graphically as the percentage of cell invasion (**D**). Data are presented as box and whisker plots from five experiments illustrating the 10th, 25th, median, 75th, and 90th percentiles. Significance was determined through comparison of the mean percentage of invasion from five experiments of cells treated with GAPDH siRNAs (46.3%) to the invasion of cells treated with MIG2 siRNAs (22.3%, one-tailed *t* test, $P < 0.05$).

cancer cells than in nonaggressive MCF-7 breast cancer cells or nontumorigenic HMECs. MIG2 mRNA was highly expressed in 30% of the breast carcinomas, and MIG2 immunoreactivity was moderate to high in 50% of the breast carcinomas tested. Among the breast carcinomas that tested positive for MIG2 immunoreactivity, slightly more than half showed strong expression. Although MIG2 expression was low or absent in the nontumorigenic HMEC lines, MIG2 was expressed in all 21 reductive mammaplasty tissues. Interestingly, we observed substantial heterogeneous staining for MIG2 among cells from a single reductive mammaplasty, whereas in cancer tissues, MIG2 was either present in most cells in the sample or absent. These results imply that the regulation of MIG2 expression could be lost in cancer cells, resulting in either negative or constitutive expression, whereas in normal cells, MIG2 is likely tightly controlled. It would be interesting to examine MIG2 expression in matched benign and malignant tissues.

MIG2 recruits the protein migfilin to cell-ECM adhesion sites and forms a complex with filamin that has been shown to be involved in controlling actin dynamics (15). The cellular

assembly of proteins at focal adhesions and the control of actin polymerization are important processes in cell migration and invasion; therefore, we investigated the role of MIG2 in TMX2-28 cell invasion. After silencing (by 52%) the expression of MIG2, we found an ~ 2 -fold decrease in TMX2-28 cell invasion, suggesting that MIG2 is involved in the invasion process. We used an established siRNA target to silence MIG2, however, we were able to achieve only a 52% decrease in MIG2 expression. This may be due to the transfection system or may be the result of MIG2 mRNA levels being highly expressed in TMX2-28 cells; therefore, studies are under way to further characterize the role of MIG2 in the invasion process.

It is reasonable to suggest that a discrepancy exists in the regulation and function of MIG2 between normal and cancer cells, and it will be important to differentiate the oncogenic role of MIG2 in breast cancer cell invasion from MIG2's role in normal breast epithelial cells. MIG2 was first identified as a serum-inducible gene, and we have shown that MIG2 is induced in HMECs following FBS stimulation. Therefore, it is plausible that in normal breast tissue, MIG2 is transcriptionally

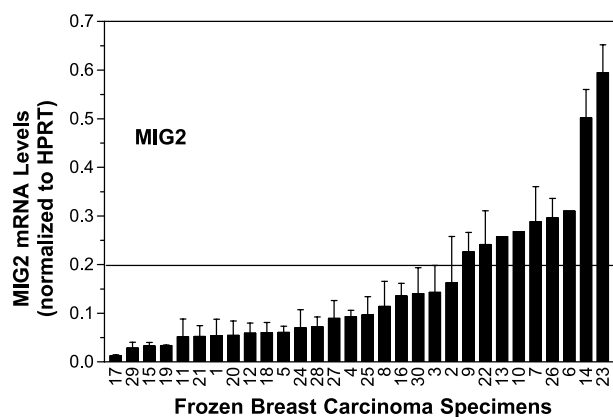


FIGURE 6. *MIG2* gene expression in human breast carcinomas. Total RNA was isolated from 30 frozen human breast tumor specimens, and gene expression was determined using real-time reverse transcription-PCR. Samples were each tested twice or thrice; SD from experimental error. Tumor specimen nos. 6, 10, and 13 were tested only once due to sample unavailability. Relative mRNA levels >0.2 arbitrary units were considered overexpressed (above the solid line).

regulated by growth factors present in the dynamic, surrounding microenvironment, whereas in HMECs in culture, *MIG2* is inducible only in response to growth factors present in the FBS. Results from several studies suggest that *MIG2* can interact with other proteins such as integrin-linked kinase and β -integrins, both of which are important cell signaling molecules that have been implicated in oncogenesis (14, 24, 25). We have reported the expression of *MIG2* in breast carcinomas and we present evidence for a role of *MIG2* in the dynamic process of cancer cell invasion.

Materials and Methods

Cell Culture, Tissue Specimens, and RNA Purification

TMX2-28 cells were kindly provided by Dr. John Gierthy (Wadsworth Center, Albany, NY). MCF-7 cells were purchased from the American Type Culture Collection (Manassas, VA), and 184, 184A1, and 184AA2 cell lines were generous gifts from Dr. Martha Stampfer (Ernest Orlando Lawrence Berkeley National Laboratory, Berkeley, CA). HMECs were purchased from Clonetics (East Rutherford, NJ) whereas MDA-MB-231, MDA-MB-435S, BT20, T47D, ZR75, and MCF-10A were obtained from the Wadsworth Center frozen stocks. TMX2-28 and MCF-7 cells were grown in DMEM (without phenol red) supplemented with 5% cosmic calf serum (Hyclone, Logan, UT), 2.0 mmol/L of L-glutamine, 0.1 mmol/L of nonessential amino acids, 10 ng/mL of insulin, 100 units/mL of penicillin, and 100 μ g/mL of streptomycin (referred to as DC₅). T47D, ZR75, BT-20, MDA-MB-231, and MDA-MB-435S cells were maintained in complete growth medium, which includes 10% FBS according to the American Type Culture Collection protocol. HMECs and MCF-10A were grown in mammary epithelial growth medium (Clonetics) which contains growth factors but no serum, whereas 184, 184A1, and 184AA2 were cultured in mammary epithelial growth medium according to Dr. M. Stampfer's protocol as posted on her web site (<http://www.lbl.gov/LBL-Programs/mrgs/>). Cells were maintained in a 37°C humidified incubator with 5% CO₂. Still-frame photo-

graphs and measurements of cell cultures were acquired with QCapture Pro 3 (Media Cybernetics, Silver Spring, MD) software. All tissue (frozen breast tumors, $n = 30$; FFPE breast tumors, $n = 34$; and FFPE reduction mammoplasty, $n = 21$) were retrieved from Baystate Medical Center, Department of Surgical Pathology and were identified numerically, maintaining patient anonymity. Institutional Review Board approval for this study was obtained from Baystate Medical Center. The 64 breast tumor samples were from primary breast carcinomas.

RNA was isolated from cell cultures with TRI Reagent (Molecular Research, Cincinnati, OH) according to the manufacturer's protocol. Isolated RNA was further purified using the Qiagen RNeasy kit with on-column DNase digestion (Qiagen, Valencia, CA). Thirty frozen breast carcinoma tissue specimens were sectioned to ≤ 0.5 cm in thickness and immediately placed in prechilled RNA Later-Ice (Ambion, Austin, TX) for 24 hours. Tissues (20-30 mg) were homogenized and RNA was isolated using the Qiagen RNeasy Fibrous Tissue kit (Qiagen).

cDNA Microarray and Real-time Reverse Transcription-PCR

RNA samples were sent to the WM Keck/Affymetrix GeneChip Resource (Yale University) for microarray analysis on the Affymetrix Human Genome U133 Plus 2.0 Array.

Real-time reverse transcription-PCR was done as previously described (26). RNA samples were reverse transcribed and amplified using the One-Step RT-PCR kit (Qiagen) in the Roche Light Cycler. Total RNA (75 ng) was incubated with Qiagen RT-PCR master mix including primers (25 μ mol/L each) and SYBR Green I nucleic acid stain (diluted 1:5,000; Molecular Probes, Eugene, OR) in precooled capillaries (Roche) and was reverse transcribed. Following reverse transcription, samples were heated, to activate the HotStarTaq DNA polymerase and to simultaneously inactivate the reverse transcriptases. The generation of amplified products was monitored over 45 PCR cycles by fluorescence of intercalating SYBR Green. Relative mRNA levels were normalized to hypoxanthine ribosyltransferase levels to control for RNA quality and concentration (27). The following gene-specific primers were designed using Primer3: *MIG2* NM_006832 AGCTTTATGAGCAGGCCAAA (nucleotide 959, sense), GAAAGGGCAGCATCAACTTC (nucleotide 1133, antisense); *Migfilin* NM_017556 CGAATGCATGGGAAGAAACT (nucleotide 1238, sense), GCAGGTTAGGAAGGGAAACC (nucleotide 1402, antisense); hypoxanthine ribosyltransferase NM_000194 ACCCCACGAAGTGTGGATA (nucleotide

Table 2. *MIG2* Expression Determined by Immunohistochemistry in Human Breast Carcinomas and Tissues from Reduction Mammoplasty

	Not discernible	Weak	Moderate	Strong
Cancer ($n = 34$)	50	23.5	11.7	14.7
Reduction mammoplasty ($n = 21$)	0	62	14.2	23.8

NOTE: Data are presented as percentages of the total (100%). Cancer tissues were examined on TMAs, and reduction mammoplasty tissues were examined on whole sections.

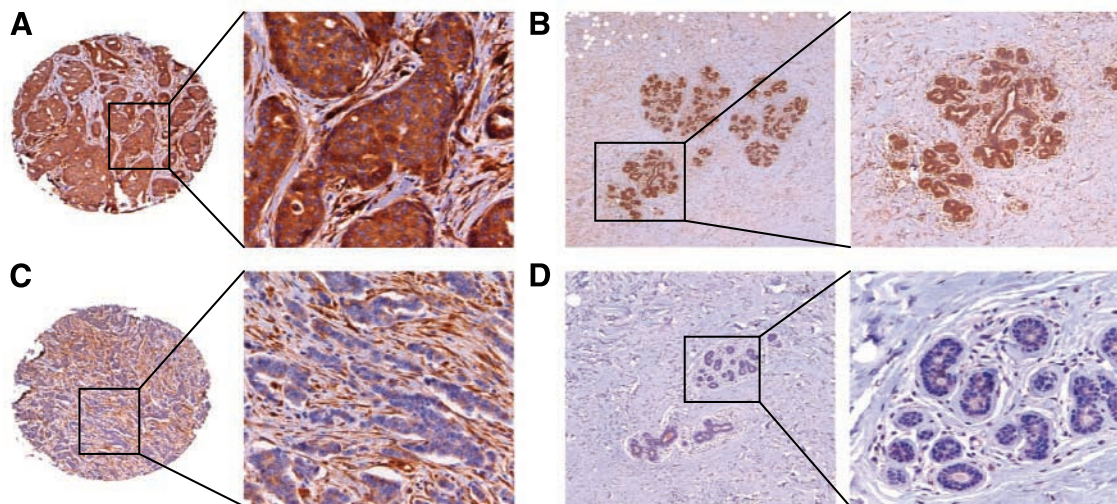


FIGURE 7. MIG2 protein expression in normal and cancer breast tissues. TMAs were constructed from 34 FFPE breast carcinomas, and tissue sections were prepared from 21 FFPE reduction mammoplasties. Protein expression was evaluated by immunohistochemistry. Representative images of MIG2 immunoreactivity in breast tumors (**A** and **C**) and reduction mammoplasties (**B** and **D**).

587, sense), AAGCAGATGGCCACAGAAGT (nucleotide 834, antisense); and β -actin NM_001101 GGAAGTTCGAGCAAGAGATGG (nucleotide 736, sense), AGCACTGTGTTGGCGTACAG (nucleotide 969, antisense).

Serum Induction

Serum induction of MIG2 was investigated following the general procedure of Wick et al. (12) in which cells seeded in standard growth medium are deprived of serum for 48 h followed by treatment with extra rich serum medium. Briefly, HMEC and MCF-7 cells were seeded in six-well plates at 5×10^4 cells/well in 2 mL of growth medium as defined above. The next day, medium was replaced with reduced medium: mammary epithelial basal medium for HMECs, and medium in which the 5% bovine calf serum was substituted with charcoal/dextran-treated FBS (Hyclone) for MCF-7 cells. After 48 h in reduced medium, cells were treated with either DC₅ (control for MCF-7), mammary epithelial growth medium (control for HMEC), medium with 10% FBS, or serum-free medium supplemented with 1 nmol/L E₂ for 4 h. RNA was isolated and gene expression was determined using real-time reverse transcription-PCR as described above.

TMA, Immunohistochemistry, and Western Immunoblotting

TMA were constructed by extracting three 1.0-mm diameter cores from each donor FFPE block and re-embedding them into a recipient paraffin block containing pre-extracted cores of paraffin spaced 1.0 mm apart. Four-micrometer sections were placed on charged slides, deparaffinized in xylene, and rehydrated in graded ethanols. Slides were rinsed in water and incubated in Citra Plus Buffer (BioGenex, San Ramon, CA) under the following conditions for antigen retrieval: micro-waving for 3 min, cooling for 1 min, heating at 98°C for 10 min, and cooling for 20 min. Immunohistochemistry was done on the Dako Autostainer using Dako Envision Plus labeled polymer-

horseradish peroxidase reagents. Anti-MIG2 mouse monoclonal antibody was diluted 1:1,000 for immunohistochemistry (15). The immunoreactivity of MIG2 was scored by a pathologist (C.N. Otis) for the intensity and the percentage of positive cells. Immunohistochemistry sections were scored on a numerical basis for both staining intensity [ranging from 0 (not discernible) to 4 (darkest staining among all controls and cases)] and the percentage of positive cells where 0, no staining; 1, <25%; 2, 25% to 50%; and 3, >75%. The score for staining intensity was multiplied by the score for the percentage of positive cells and the products were separated into four groups: no staining, weak, moderate, and strong staining.

Cell cultures were lysed with prechilled SDS buffer (1% SDS, 0.06 mol/L Tris-HCl, and 10% glycerol), and cell extracts were used for Western immunoblotting. Protein lysates (10 μ g) were mixed with NuPage sample buffer and reducing agent (Invitrogen, Carlsbad, CA), and then heated at 70°C for 10 min. Protein lysates were then separated on a 10% Tris-HCl polyacrylamide gel (Bio-Rad, Hercules, CA) using the Mini-Protein 3 cell (Bio-Rad) according to the manufacturer's protocol. Separated proteins were transferred to an Immuno-Blot polyvinylidene difluoride membrane (Bio-Rad) using the Mini Trans-Blot electrophoretic transfer cell and protocol (Bio-Rad). Membranes were incubated in blocking buffer (5% nonfat dry milk/TBS and 0.1% Tween 20) for 30 min at room temperature with gentle shaking. The membrane was then incubated with the primary antibody overnight at 4°C, and with the appropriate secondary antibodies, either anti-rabbit IgG horseradish peroxidase-linked antibodies (1:1,000, Cell Signaling Technology, Beverly, MA) or anti-mouse IgG horseradish peroxidase-linked antibodies (1:5,000, Santa Cruz Biotechnology, Santa Cruz, CA), for 1 h at room temperature. Chemiluminescent signals were detected with the SuperSignal West Pico kit and protocol (Pierce, Rockford, IL). Anti-MIG2 mouse monoclonal antibody (15) was diluted 1:10,000 for Western immunoblotting, and β -actin 1:1,000 (Cell Signaling Technology).

Matrigel Invasion Assay

BD BioCoat Matrigel Invasion Chambers (Discovery Labware, Bedford, MA) and 8.0- μ m pore size PET track-etched membranes (Becton Dickinson, San Diego, CA) were used for the invasion assay according to the manufacturer's protocol (Discovery Labware). Cells (100,000-150,000 cells/mL) were plated in the top chamber in DMEM and culture medium with 5% FBS (Hyclone) was used in the bottom chamber as a chemoattractant. Twenty-four hours later, cells were fixed and stained using the HEMA 3 STAT Pack (Fisher Scientific). Cell number was counted on microphotographs taken over five areas of the membrane.

RNA Interference

The siRNA target for MIG2 was adapted from the literature (target sequence 5'-AACAGCGAGAATCTTGAGGC-3'; ref. 15). siRNA templates for MIG2 were designed using the Ambion Web-based design tool, whereas the template for the GAPDH-siRNAs was supplied with the siRNA construction kit from Ambion. The siRNA construction kit (Ambion) was used for *in vitro* transcription of siRNAs. siRNAs (10 nmol/L) were mixed with siPORT NeoF \times lipid-based agent for reverse transfection (2 μ L/well; Ambion) and then overlaid with 9×10^4 cells per well (12-well plate; 4 cm²/well) for transfection. After 24 h, medium containing the transfection complexes was replaced with fresh complete growth medium to minimize cellular toxicity, and cells were incubated for an additional 24 h. Following a total of 48 h, cells were washed with PBS, collected with trypsinization, and used in the invasion assay as described above.

Statistical Analyses

Data were analyzed and graphed with GraphPad Prism version 3.02 (GraphPad Software, Inc., San Diego, CA). For ANOVA and post hoc comparisons, significance was set at $P < 0.05$. Associations between MIG2 mRNA level and tumor grade, and immunoreactivity of MIG2 antibody and tumor grade were evaluated by χ^2 test with significance set at $P < 0.05$.

References

- Hanahan D, Weinberg RA. The hallmarks of cancer. *Cell* 2000;100:57-70.
- Weir HK, Thun MJ, Hankey BF, et al. Annual report to the nation on the status of cancer, 1975-2000, featuring the uses of surveillance data for cancer prevention and control. *J Natl Cancer Inst* 2003;95:1276-99.
- Solomayer EF, Diel IJ, Meyberg GC, Gollan C, Bastert G. Metastatic breast cancer: clinical course, prognosis and therapy related to the first site of metastasis. *Breast Cancer Res Treat* 2000;59:271-8.
- Cairns RA, Khokha R, Hill RP. Molecular mechanisms of tumor invasion and metastasis: an integrated view. *Curr Mol Med* 2003;3:659-71.
- Chambers AF, Groom AC, MacDonald IC. Dissemination and growth of cancer cells in metastatic sites. *Nat Rev Cancer* 2002;2:563-72.
- Minn AJ, Gupta GP, Siegel PM, et al. Genes that mediate breast cancer metastasis to lung. *Nature* 2005;436:518-24.
- Friedl P, Wolf K. Tumour-cell invasion and migration: diversity and escape mechanisms. *Nat Rev Cancer* 2003;3:362-74.
- Liotta LA, Stetler-Stevenson WG. Tumor invasion and metastasis: an imbalance of positive and negative regulation. *Cancer Res* 1991;51:5054-9s.
- Sahai E. Mechanisms of cancer cell invasion. *Curr Opin Genet Dev* 2005;15:87-96.
- Wang W, Goswami S, Sahai E, Wyckoff JB, Segall JE, Condeelis JS. Tumor cells caught in the act of invading: their strategy for enhanced cell motility. *Trends Cell Biol* 2005;15:138-45.
- Wolf K, Mazo I, Leung H, et al. Compensation mechanism in tumor cell migration: mesenchymal-amoeboid transition after blocking of pericellular proteolysis. *J Cell Biol* 2003;160:267-77.
- Wick M, Burger C, Brusselbach S, Lucibello FC, Muller R. Identification of serum-inducible genes: different patterns of gene regulation during G0-S and G1-S progression. *J Cell Sci* 1994;107:227-39.
- Weinstein EJ, Bournier M, Head R, Zakeri H, Bauer C, Mazzarella R. URP1: a member of a novel family of PH and FERM domain-containing membrane-associated proteins is significantly over-expressed in lung and colon carcinomas. *Biochim Biophys Acta* 2003;1637:207-16.
- Kloeker S, Major MB, Calderwood DA, Ginsberg MH, Jones DA, Beckerle MC. The Kindler syndrome protein is regulated by transforming growth factor- β and involved in integrin-mediated adhesion. *J Biol Chem* 2004;279:6824-33.
- Tu Y, Wu S, Shi X, Chen K, Wu C. Migfilin and Mig-2 link focal adhesions to filamin and the actin cytoskeleton and function in cell shape modulation. *Cell* 2003;113:37-47.
- Gkretsi V, Zhang Y, Tu Y, et al. Physical and functional association of migfilin with cell-cell adhesions. *J Cell Sci* 2005;118:697-710.
- Fasco MJ, Amin A, Pentecost BT, Yang Y, Gierthy JF. Phenotypic changes in MCF-7 cells during prolonged exposure to tamoxifen. *Mol Cell Endocrinol* 2003;206:33-47.
- Pentecost BT, Bradley LM, Gierthy JF, Ding Y, Fasco MJ. Gene regulation in an MCF-7 cell line that naturally expresses an estrogen receptor unable to directly bind DNA. *Mol Cell Endocrinol* 2005;238:9-25.
- Liu G, Loraine AE, Shigeta R, et al. NetAffx: Affymetrix probesets and annotations. *Nucleic Acids Res* 2003;31:82-6.
- Coussens LM, Fingleton B, Matrisian LM. Matrix metalloproteinase inhibitors and cancer: trials and tribulations. *Science* 2002;295:2387-92.
- Eckhardt BL, Parker BS, van Laar RK, et al. Genomic analysis of a spontaneous model of breast cancer metastasis to bone reveals a role for the extracellular matrix. *Mol Cancer Res* 2005;3:1-13.
- Wang W, Goswami S, Lapidus K, et al. Identification and testing of a gene expression signature of invasive carcinoma cells within primary mammary tumors. *Cancer Res* 2004;64:8585-94.
- Kato K, Shiozawa T, Mitsushita J, et al. Expression of the mitogen-inducible gene-2 (mig-2) is elevated in human uterine leiomyomas but not in leiomyosarcomas. *Hum Pathol* 2004;35:55-60.
- Brakebusch C, Bouvard D, Stanchi F, Sakai T, Fassler R. Integrins in invasive growth. *J Clin Invest* 2002;109:999-1006.
- Sepulveda JL, Gkretsi V, Wu C. Assembly and signaling of adhesion complexes. *Curr Top Dev Biol* 2005;68:183-225.
- Gozgit JM, Nestor KM, Fasco MJ, Pentecost BT, Arcaro KF. Differential action of polycyclic aromatic hydrocarbons on endogenous estrogen-responsive genes and on a transfected estrogen-responsive reporter in MCF-7 cells. *Toxicol Appl Pharmacol* 2004;196:58-67.
- de Kok JB, Roelofs RW, Giesendorf BA, et al. Normalization of gene expression measurements in tumor tissues: comparison of 13 endogenous control genes. *Lab Invest* 2005;85:154-9.